2024 European Control Conference (ECC)
June 25-28, 2024. Stockholm, Sweden

An approach to multi-energy network modeling by multilinear models

Leandro Samaniego[1,3], Enrico Uhlenberg[3], Christoph Kaufmann[2], Marah Engels[1], Georg Pangalos[2], Carlos Cateriano Yáñez[2,3,4] and Gerwald Lichtenberg[3].

Abstract— **Multilinear time-invariant (MTI) models are a mathematical framework to represent and analyze high-dimensional nonlinear systems. Tensor decomposition techniques are used to improve computational efficiency and reduce storage effort. Applications of large-scale multi-energy systems can benefit from novel methodologies, such as modeling power systems using semi-explicit and fully implicit differential-algebraic equations. The multilinear modeling framework is embedded in a new MTI-toolbox suitable for multi-energy networked systems. The modeling framework and MTI-toolbox is demonstrated by an interconnected medium-size power system network, comprised of small three bus subsystems.**

I. INTRODUCTION

The modern power grid stands as a critical backbone of our society, facilitating the reliable delivery of electricity to meet the demands of our technologically advanced world. Power system modeling is crucial for maintaining stability, security, and optimal operation of these intricate networks. With the integration of renewable energy sources, the necessity for more accurate, efficient, and scalable modeling techniques becomes increasingly apparent. However, the rapid expansion of renewables and distributed generation has introduced variability and uncertainty, [1], [2], challenging traditional modeling approaches and resulting in suboptimal operation, [3], [4]. Consequently, there is a pressing need for the development of new modeling and control techniques capable of accommodating renewable energies effectively.

Multilinear time-invariant theory is an active field of research for its promising potential to capture complex dynamics of distributed large-scale systems, such us multi-energy renewable energy networks. With the development of innovative modeling and model-based controller strategies, [5]–[7], MTI modeling offers a new avenue for standardized techniques and algorithms to analyze and regulate systems of great complexity. The equations describing multi-energy systems can be adapted to fit the MTI framework, where the dynamics are described through tensor operations, opening the door to several tensor applications. Of significant importance, is the techniques of tensor rank reduction, where large multidimensional data tensor structures can be approximated with a significant reduction in storage effort, provided the approximation is reachable.

This paper centers on the representation of a complex power system within the MTI modeling framework, where dynamics are captured through implicit sets of equations. Subsequently, these representations are compared with the original nonlinear model. The techniques employed in this study hold promise for modeling multi-energy systems formed by various components such as wind and solar energies, battery energy storage, heat storage and exchangers, and gas turbines. These components cane be described by potentially implicit sets of differential equations This is the case of power systems, which can be also be specified in terms of differential algebraic equations (DAEs), [8]–[10]. Making the connection between MTI models and DAEs opens the door for tensor algebra approaches towards a much richer and standardized class of power system models.

The authors of this paper are aware of the complexity in solving DAEs using numerical integration methods such as Backward Differentiation Formulas or Runge-Kutta, [11]. The notion of indexes, [12], characterizes and offers a measure of the system's ease of numerical solvability, is central in the theory of DAEs. In the context of MTI models, the study of overdetermined and underdetermined sets of DAEs, [13], and index topics are left for future research. This paper deals only with the so-called index-1 systems.

In order to facilitate the development and computation of MTI models a novel toolbox for use in Matlab® was created. The MTI-Toolbox is a collection of functions and classes that allow the user to create, manipulate and simulate MTI models without the need of in-depth knowledge of the underlying tensor algebra.

In this paper, an implicit MTI model of a medium-sized nine bus power network is given, and a simulation using Matlab® and Simulink® is used to compare it to a nonlinear model.

II. MULTILINEAR MODELS

In this section a description of multilinear models is first given in the context of tensor operations. Then the Boolean and implicit multilinear model classes are introduced.

A. Tensor representation

A tensor $\mathsf{X} \in \mathbb{R}^{I_1 \times I_2 \times \cdots \times I_N}$ is an N-dimensional arrangement of elements, its entries are denoted by $x(i_1, i_2, \ldots, i_N)$,

[1] Leandro Samaniego and Marah Engels are with Competence Center for Renewable Energies and Energy Efficiency, HAW Hamburg, Germany. {Leandro.SamaniegoVallejos;marah.engels}@haw-hamburg.de

[2] Christoph Kaufmann, Georg Pangalos and Carlos Cateriano Yáñez are with the Application Center for Integration of Local Energy Systems, Fraunhofer IWES, Hamburg, Germany. {christoph.kaufmann;georg.pangalos}@iwes.fraunhofer.de

[3] Leandro Samaniego, Enrico Uhlenberg, Carlos Cateriano Yáñez and Gerwald Lichtenberg are with the Faculty of Life Sciences, HAW Hamburg, Germany. {Enrico.Uhlenberg;gerwald.lichtenberg}@haw-hamburg.de

[4] Carlos Cateriano Yáñez is with the University Institute of Automation and Industrial Informatics, Universitat Politècnica de València, Valencia, Spain. carlos.cateriano.yanez@iwes.fraunhofer.de

where the indexes $i_j \in \{1, 2, \dots, I_j\}$ belong to each dimension out of $j = 1, \dots, N$. A tensor of dimension two is a matrix and a tensor of dimension one is a vector. The relation between tensors, multilinear functions and multilinear state space models was introduced in [14]. In an MTI model the state transition is computed using a contracted product [15]. The contracted product operation between a tensor $\mathsf{X} \in \mathbb{R}^{I_1\times\cdots\times I_N\times J_1\times\cdots\times J_M}$ and a tensor $\mathsf{Y} \in \mathbb{R}^{I_1\times\cdots\times I_N}$ is defined as

$$\mathsf{Z} = \langle \mathsf{X} | \mathsf{Y} \rangle \in \mathbb{R}^{J_1\times\cdots\times J_N}.$$

with elements

$$z(j_1, \dots, j_M) \\ = \sum_{i_1=1}^{I_1} \cdots \sum_{i_N=1}^{I_N} y(i_1, \dots, i_N) x(i_1, \dots, i_N, j_1, \dots, j_M).$$

The state equations with inputs $\mathbf{u} \in \mathbb{R}^m$ and states $\mathbf{x} \in \mathbb{R}^n$ are then written as

$$\dot{\mathbf{x}} = \langle \mathsf{F} | \mathsf{M}(\mathbf{x}, \mathbf{u}) \rangle, \tag{1}$$

where $\mathsf{F} \in \mathbb{R}^{\overbrace{2\times\cdots\times 2}^{n+m}\times n}$ is the state transition tensor. The monomial tensor $\mathsf{M}(\mathbf{x}, \mathbf{u}) \in \mathbb{R}^{\overbrace{2\times\cdots\times 2}^{n+m}}$ consist of all possible combinations of the components in $\mathbf{x}$ and $\mathbf{u}$. Explicit MTI systems written as (1) are referred as eMTI. As an example, the state equation of an eMTI system with two states is given by

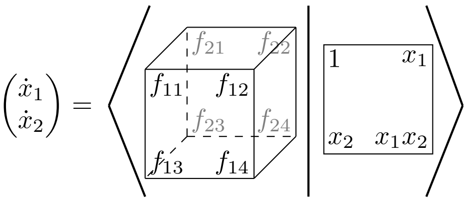

$$\begin{pmatrix}\dot x_1\\ \dot x_2\end{pmatrix} = \begin{pmatrix} f_{11} + f_{12}x_1 + f_{13}x_2 + f_{14}x_1x_2 \\ f_{21} + f_{22}x_1 + f_{23}x_2 + f_{24}x_1x_2 \end{pmatrix}.$$

B. Implicit representation

Implicit multilinear time-invariant (iMTI) models were introduced in [15], they are sets of implicit multilinear equations, where the state derivatives $\dot{\mathbf{x}}$ are also present in the equations along with the states $\mathbf{x}$ and inputs $\mathbf{u}$.

The state equations of an iMTI are also written with the contracted product

$$\langle \mathsf{H} | \mathsf{M}(\dot{\mathbf{x}}, \mathbf{x}, \mathbf{u}) \rangle = \mathbf{0}, \tag{2}$$

where $\mathsf{H} \in \mathbb{R}^{\overbrace{2\times\cdots\times 2}^{2n+m}\times e}$ is the parameter tensor, e is the total number of equations in the system and $\mathsf{M}(\dot{\mathbf{x}}, \mathbf{x}, \mathbf{u})$ is an augmented version of the monomial tensor in (1).

The iMTI modeling class can include algebraic variables in the system equations, turning a set of implicit ordinary differential equations into a set of DAEs. To describe DAEs the model is augmented with an additional vector of algebraic variables $\mathbf{z} \in \mathbb{R}^{n_z}$ in the monomial tensor, leading to the formulation

$$\langle \mathsf{H} | \mathsf{M}(\dot{\mathbf{x}}, \mathbf{x}, \mathbf{u}, \mathbf{z}) \rangle = \mathbf{0}. \tag{3}$$

A special class of DAEs which commonly arises in electrical circuit modeling and many other applications, [16]–[18], is the semi-explicit class, where (3) can be re-written as

$$\mathbf{E}\dot{\mathbf{x}} = \langle \mathsf{F} | \mathsf{M}(\mathbf{x}, \mathbf{u}, \mathbf{z}) \rangle, \tag{4}$$

here the mass matrix $\mathbf{E} \in \mathbb{R}^{(n+n_z)\times n}$ defines n_z algebraic equations by setting the derivatives to zero. The semi-explicit multilinear (sMTI) class was introduced in [19], in the context of modeling AC power systems comprised of voltage source converters.

The example presented in section IV of this paper is an iMTI model, however it can also be expressed as a sMTI, as is typical for electric systems. The iMTI model is used because the MTI-toolbox is developed to handle the more general fully implicit models.

C. Boolean functions

All Boolean functions belong to the class of multilinear functions, [20]. Boolean functions operate on binary sets, where its variables assume two-element values as $B = \{0, 1\}$ or $B = \{\text{True}, \text{False}\}$. Boolean functions of n variables can be represented by truth vectors of 2^n elements, $\mathbf{b} \in \mathbb{B}^{2^n}$. Boolean functions of $\mathbf{x} \in \mathbb{B}^n$ variables, expressed within the multilinear framework are written as the inner product of $\mathbf{b}^{\mathrm{T}} \in \mathbb{B}^{2^n}$ with a vector of literals $\mathbf{l}(\mathbf{x}) \in \mathbb{R}^{2^n}$, as

$$f(\mathbf{x}) = \mathbf{b}^{\mathrm{T}}\mathbf{l}(\mathbf{x}),$$

where

$$\mathbf{l}(\mathbf{x}) = \begin{pmatrix} 1 - x_n \\ x_n \end{pmatrix} \otimes \cdots \otimes \begin{pmatrix} 1 - x_1 \\ x_1 \end{pmatrix} \in \mathbb{R}^{2^n},$$

and $\otimes$ denotes the Kronecker product.

III. Tensor decomposition

As the number of variables in a system, including states and inputs, increases, so does the size of the tensor needed for representation. As a result, the amount of data necessary to fully describe the tensors grows rapidly, increasing computational complexity and storage requirements. For example, to fully describe the model in (3), the storage effort requires

$$\zeta_{full}(\mathsf{H}) = e2^{2n+m+n_z},$$

elements to be stored.

Using decomposed or factorized tensors instead of full tensors allows to alleviate the storage demand by providing a compact representation of high-dimensional tensors, [21]. Tensors represented in the canonic polyadic (CP) decomposition, factorize into a sum of r outer products of vectors, where the smallest possible r is the so-called tensor rank, [21]. In the CP decomposition the monomial tensor $\mathsf{M}(\dot{\mathbf{x}}, \mathbf{x}, \mathbf{u}, \mathbf{z})$ from (3) is rank-1 by construction, [15], while the parameter tensor H can have an arbitrary rank r, and it is decomposed in of $2n + m + n_z + 1$ factor matrices.

The storage effort to describe the model in (3) using the CP format requires

$$\zeta_{CP}(\mathsf{H}) = (2(2n + m + n_z) + e)r, \tag{5}$$

elements to be stored.

In this paper tensors are represented as CP-normalized or CPN, which is a reduced format aimed to further improve the storage cost of a CP tensor. By applying a 1-norm to the columns of the factor matrices of tensor H, it is possible to store and represent a multilinear model with two matrices. A matrix $\mathbf{H}_s \in \mathbb{R}^{(2n+m+n_z)\times r}$ describes the combination of state derivatives, states and inputs present in the model equations. A matrix $\mathbf{H}_\phi \in \mathbb{R}^{e\times r}$ contains the structure and coefficients off all terms present in the model equations. The manner to compute the 1-norm CPN (CPN1) decomposition from a CP tensor H is presented in [15].

The implicit equations in (3) are obtained from $\mathbf{H}_s$ and $\mathbf{H}_\phi$, by applying

$$\sum_{k=1}^{r} \mathbf{H}_\phi(:,k) \prod_{i=1}^{N} (1 - |\mathbf{H}_s(i,k)| + \mathbf{H}_s(i,k)\boldsymbol{\mu}(i)) = \mathbf{0}, \tag{6}$$

where $\boldsymbol{\mu} = (\dot{x}_1, \dots, \dot{x}_n, x_1, \dots, x_n, u_1, \dots, u_m, z_1, \dots, z_{n_z})$ contains the state derivatives, states and inputs and $N = 2n + m + n_z$.

As mentioned, the MTI-Toolbox enables the construction and computation of implicit and explicit MTI systems, utilizing the CPN1 decomposition internally. To facilitate working with existing models, the toolbox implements several functions to approximate MTI representations from existing Simulink® models, time series data or CP tensors.

IV. Power system network example

In this section, a power system example from the literature is presented. An iMTI model formulated directly as a decomposed CPN1 tensor for the example is presented. Finally, the simulation results are presented.

A. Three bus model

A three bus network from literature is now introduced, it serves as the building block of the example in this paper. The three bus network model was presented in [22], [23], for experimental model verification. It consists of a network with a nominal frequency of 50 Hz and a nominal voltage of 310 V at the nodes. The generation at the nodes is done by voltage source DC-AC inverters and the loads are purely resistive.

The network modeling is done in a common global rotating DQ-frame which belongs to one single inverter. Each of the remaining inverters is modeled in their local rotating dq-frame. The remaining inverters can be translated to the global DQ-frame by a rotation matrix, [24].

Fig. 1 depicts a single inverter scheme while Fig. 2 depicts the three bus network, where the injected currents from the inverters into the network are symbolized by $\mathbf{i}_{\mathrm{oDQ}_j}$, and bus voltages are symbolized by $\mathbf{v}_j$, for $j = 1, 2, 3$.

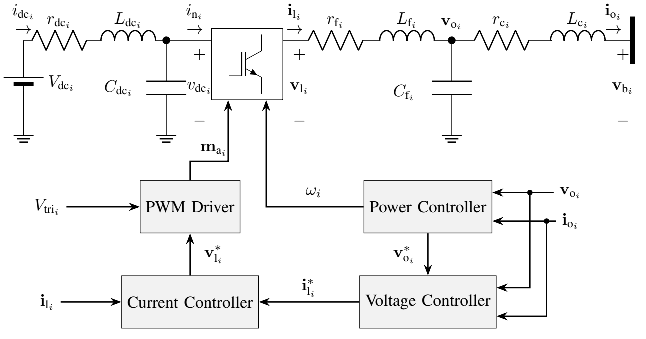
i_{dc_i}
r_{dc_i}
L_{dc_i}
i_{n_i}
$\mathbf{i}_{\mathrm{l}_i}$
r_{f_i}
L_{f_i}
$\mathbf{v}_{\mathrm{o}_i}$
r_{c_i}
L_{c_i}
$\mathbf{i}_{\mathrm{o}_i}$
V_{dc_i}
C_{dc_i}
v_{dc_i}
$\mathbf{v}_{\mathrm{l}_i}$
C_{f_i}
$\mathbf{v}_{\mathrm{b}_i}$
$\mathbf{m}_{\mathrm{a}_i}$
V_{tri_i}
PWM Driver
ω_i
Power Controller
$\mathbf{v}_{\mathrm{o}_i}$
$\mathbf{i}_{\mathrm{o}_i}$
$\mathbf{v}^*_{\mathrm{l}_i}$
$\mathbf{v}^*_{\mathrm{o}_i}$
$\mathbf{i}_{\mathrm{l}_i}$
Current Controller
$\mathbf{i}^*_{\mathrm{l}_i}$
Voltage Controller

Fig. 1. Inverter scheme, [23].

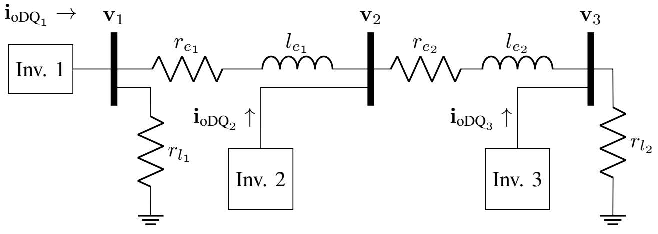

Fig. 2. Three bus network, [22].

Each inverter in the network has fifteen states, comprised of powers, currents, voltages, controller states among others, see [22], [23]. A single inverter state vector is written as $\mathbf{x}_{\mathrm{I}_i} = [\mathbf{i}_{\mathrm{dc}_i}, \mathbf{v}_{\mathrm{dc}_i}, \cdots, \mathbf{v}_{\mathrm{o}_i}, \mathbf{i}_{\mathrm{o}_i}]^{\mathrm{T}}$. The states of all inverters in a network are stacked together. For the three bus system, that is

$$\mathbf{x}_{\mathrm{I}} = [\mathbf{x}_{\mathrm{I}_1}^{\mathrm{T}}, \mathbf{x}_{\mathrm{I}_2}^{\mathrm{T}}, \mathbf{x}_{\mathrm{I}_3}^{\mathrm{T}}]^{\mathrm{T}}. \tag{7}$$

The equations describing the dynamics of the inverters and node voltages $\mathbf{v}$ of the network are

$$\dot{\mathbf{x}}_{\mathrm{I}} = \mathbf{f}_{\mathrm{I}}(\mathbf{x}_{\mathrm{I}}, \mathbf{v}). \tag{8}$$

Here $\mathbf{f}_{\mathrm{I}}$ is nonlinear with reciprocal and trigonometric functions, see [23] for more details.

In the following section an implicit model with algebraic constraints is derived for an augmented version of the three bus system.

B. Implicit multilinear model

In [25], a medium size network is created out of interconnected three bus units in a ring arrangement to make the overall example. The scheme is depicted here in Fig. 3; the network is made up of nine buses, where each block has the same structure as in Fig. 2. There are nine lines between nodes, including the lines connecting the blocks in Fig. 3, these are lines three, six and nine. Also in the network, there are six loads at busses one, three, four, six, seven, and nine. The parameters of all blocks are equal.

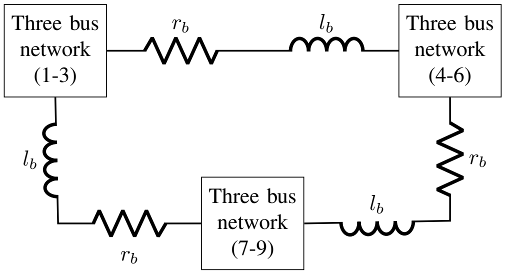

Fig. 3. Nine bus power system.

In order to represent the network state evolution as an iMTI model, $\mathbf{f}_\mathrm{I}$ must be modified into the multilinear modeling class. This is done by introducing algebraic variables $\mathbf{z}_\mathrm{dc}$ to substitute certain nonlinear relationships. For example, writing down the equations of the DC side in Fig. 1 yields reciprocal relationships between the average active power P_i and input voltage v_{dc_i} of a single inverter. That is,

$$\frac{\mathrm{d}}{\mathrm{d}t} v_{\mathrm{dc}_i} = \frac{1}{C_{\mathrm{dc}_i}} i_{\mathrm{dc}_i} - \frac{P_i}{C_{\mathrm{dc}_i} v_{\mathrm{dc}_i}}. \tag{9}$$

The nonlinearity can be substituted by adding additional algebraic variables and constraints. For a single inverter, this yields

$$\begin{aligned} \frac{\mathrm{d}}{\mathrm{d}t} v_{\mathrm{dc}_i} &= \frac{1}{C_{\mathrm{dc}_i}} i_{\mathrm{dc}_i} - \frac{P_i z_{\mathrm{dc}_i}}{C_{\mathrm{dc}_i}}, \\ 0 &= z_{\mathrm{dc}_i} v_{\mathrm{dc}_i} - 1. \end{aligned} \tag{10}$$

This transforms (9) into a set of DAEs above, where the only nonlinearities present fall within the iMTI modeling class. Since the substitution added one new variable and one new equation the overall set remains regular.

Trigonometric functions are included in the equations too. These fall from the rotation matrix mentioned in section IV-A. Dealing with cosine and sine functions, a variable substitution as $\mathbf{x}_{\mathrm{t}_i} := [x_{\mathrm{t1}_i}, x_{\mathrm{t2}_i}]^T = [\cos(\delta_i), \sin(\delta_i)]^T$, can be applied. Here δ_i is the angular position of any inverter i in its local dq-frame.

Because this substitution adds two variables, two additional equations,

$$\frac{\mathrm{d}}{\mathrm{d}t} \mathbf{x}_{\mathrm{t}_i} = \begin{bmatrix} \dot{x}_{\mathrm{t1}_i} \\ \dot{x}_{\mathrm{t2}_i} \end{bmatrix} = \dot{\delta}_i \begin{bmatrix} -x_{\mathrm{t2}_i} \\ x_{\mathrm{t1}_i} \end{bmatrix}, \tag{11}$$

are used to describe how these variables change over time. An additional restriction on $\mathbf{x}_{\mathrm{t}_i}$ would impose that its components behave as trigonometric functions; this may be

$$|\mathbf{x}_{\mathrm{t}_i}|_2^2 = x_{\mathrm{t1}_i}^2 + x_{\mathrm{t2}_i}^2 = \cos(\delta_i)^2 + \sin(\delta_i)^2 = 1. \tag{12}$$

It is simple to turn this equation into multilinear restrictions by adding yet two additional variables for each square term. However, the problem is that (12) doesn't introduce any new variables, resulting in an overdetermined system of equations, which Matlab® implicit solvers cannot address. For this reason, equation (12) is not included in the final set of DAEs. The component variables of $\mathbf{x}_{\mathrm{t}_i}$ must be monitored to fulfil (12), when the restriction don't hold, the simulation results become no longer valid. It has been noted that restrictions may deviate over time due to numerical errors, potentially leading to a significant compounding error, especially during extended simulation periods. Another alternative is for all trigonometric functions in $\mathbf{f}_\mathrm{I}$ to be linearized around an equilibrium point, as illustrated in [22].

The network-load equations are obtained by following the work presented in [26], [27], where the power network is viewed as a graph with $|\mathcal{V}|$ nodes of voltage $\mathbf{v}$ and $|\mathcal{E}|$ edges with line currents $\mathbf{i}$. Combining the modified inverter equations with the network load equations for the nine bus system yields,

$$\begin{aligned} \dot{\mathbf{x}}_\mathrm{I} &= \mathbf{g}_\mathrm{I}(\mathbf{x}_\mathrm{I}, \mathbf{x}_\mathrm{t}, \mathbf{v}, \mathbf{z}_{dc}), \\ \mathbf{L}\frac{\mathrm{d}}{\mathrm{d}t}\mathbf{i} &= -(\mathbf{R} + \mathbf{L}\boldsymbol{\mathcal{W}}_\mathbf{i}(\omega_1))\mathbf{i} + \mathbf{B}^\mathrm{T}\mathbf{v}, \\ \mathbf{v} &= \mathbf{R}_N\big(\mathbf{i}_\mathrm{oDQ} - \mathbf{G}_\mathrm{L}\mathbf{v} - \mathbf{B}\mathbf{i}\big), \end{aligned} \tag{13}$$

where $\mathbf{x}_\mathrm{I}$ now holds the states for the nine inverters, $\mathbf{L}, \mathbf{R}$ hold the transmission line parameters, $\mathbf{G}_\mathrm{L}$ holds the conductivity of the loads, $\mathbf{B}$ is a node-edge oriented incidence matrix that represents the network graph, $\mathbf{R}_N$ models virtual resistors to ground at each node, ensuring that the node voltages are defined and properly conditioned for numerical solution, [23]. The skew-symmetric matrix $\boldsymbol{\mathcal{W}}_\mathbf{i}(\omega_1)$ is an additional term that accounts for equations based on the rotating DQ-frame. The global frequency of the network ω_1, is dictated by the inverter in bus one of the network. This frequency is the rotation rate of the global DQ-frame. As mentioned, all inverter values can either be referenced in the local dq-frame or global DQ-frame.

Equations (13) can be augmented into a hybrid model by introducing Boolean variables. For this example the conductivity matrix $\mathbf{G}_\mathrm{L}$ is set to vary during the simulation. The change in conductivity occurs gradually following a ramp function $u(t)$. A ramp function can be created with the boolean variables

$$\begin{aligned} x_{\mathrm{b}_l} &= \sigma(t - t_l), \\ x_{\mathrm{b}_u} &= \sigma(t - t_u), \end{aligned} \tag{14}$$

here σ is the Heaviside function and t_l and t_u are the lower and upper bounds of time window where the conductivity change takes place. The conductivity and ramp functions can be defined within the MTI framework as

$$\begin{aligned} \mathbf{G}_\mathrm{L}(u) &= u\mathbf{G}_{\mathrm{L}_l} + (1-u)\mathbf{G}_{\mathrm{L}_u}, \\ u(t) &= (1 - x_{\mathrm{b}_l})u_l + x_{\mathrm{b}_l}(1 - x_{\mathrm{b}_u})((t - t_l)s + u_l) \\ &\quad + x_{\mathrm{b}_u}u_u, \end{aligned} \tag{15}$$

where $\mathbf{G}_{\mathrm{L}_l}$ and $\mathbf{G}_{\mathrm{L}_u}$ are the transition conductivity values. The ramp decreases from $u_l = 1$ to $u_u = 0$ while transitioning with a slope of $s = (-1)/(t_u - t_l)$.

Combining (13), (14) and (15) leads to a hybrid model, since both, real valued and Boolean variables, are used.

C. Implementation and simulation setup

The equations of the nine bus system are comprised of 198 variables and $e = 198$ equations, with $n = 171$ differentiable variables $\mathbf{x}$, a single input $m = 1$, and $n_z = 27$

algebraic variables $\mathbf{z}$. The number of distinct terms within the equations, encompassing variables and their combinations, holds significant importance as it establishes an upper limit on the rank of the model tensor. For this example the total number of unique terms is 651.

To simulate the complete system, the equations in (13) are represented in the iMTI class as

$$\langle \mathsf{H}_{9b} | \mathsf{M}(\dot{\mathbf{x}}, \mathbf{x}, \mathbf{u}, \mathbf{z}) \rangle = \mathbf{0}, \tag{16}$$

where the differential variables are $\mathbf{x} = [\mathbf{x}_{\mathrm{I}}^{\mathrm{T}}, \mathbf{i}^{\mathrm{T}}, \mathbf{x}_{\mathrm{t}}^{\mathrm{T}}]^{\mathrm{T}}$, and the algebraic variables are $\mathbf{z} = [\mathbf{v}^{\mathrm{T}}, \mathbf{z}_{\mathrm{dc}}^{\mathrm{T}}]^{\mathrm{T}}$. This DAE system has a differentiation index one and can be solved using Matlab® implicit solvers.

In order to create the model, first, all the variables are declared as symbolic, with their corresponding dimensions and labels in Matlab® workspace. The model equations of the nine bus system are then built through vectorized relationships following (13). Once the model is available, a wrapper function from the MTI-toolbox can be used to create the CP tensor object H_{9b}. A CPN1 representation is then obtained using another normalization wrapper function from the toolbox. From the CPN1 representation, the relation in (6) can be used to create a function handle for the implicit solver $ode15i$ in Matlab®. The solver receives an additional function handle parameter to model $u(t)$ in (15). The setup of the implicit solver, assigning the function handles and initial conditions are done manually for this work. When using the MTI-Toolbox, wrapper classes are available to automate this process and to provide a more user-friendly interface.

The parameters and initial conditions in [19], [20] are used as a reference for the nine bus system in Fig. 3. However, Matlab®/Simulink® is used to acquire a complete set of consistent initial conditions and a steady-state operating point using the Simscape Electrical libraries and tools. The simulation is done over a time span of $0 \leq t \leq 1\,\mathrm{s}$, at $t = 0.3\,\mathrm{s}$, the values of the loads in busses one and nine are increased by $20\,\%$, while decreased by $40\,\%$ in bus four. The changes occur gradually in the conductivity matrix $\mathbf{G}_{\mathrm{L}}(u)$ over a time span of $\Delta t = 0.001\,\mathrm{s}$, where the ramp function $u(t)$ is used to model the load changes.

D. Results

The figures below show a comparison of the nonlinear and iMTI models. Because the simulation's goal is to assess how well the iMTI model performs against the nonlinear model, the network operating conditions may be suboptimal. However, future research on this topic may include a more careful examination of operation and the constraints that this may impose.

Fig. 4 depicts the active power output of the inverters at busses one, four and nine, symbolized as P_1, P_4, P_9. It can be observed that both models have similar values overall.

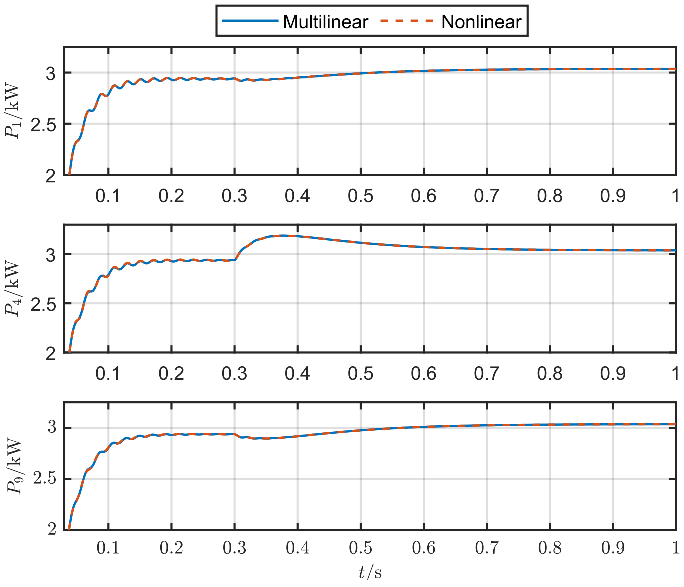

Fig. 4. Active power supplied by inverters at busses one, four and nine.

Fig. 5 shows the current between busses four and five in the DQ-frame, here symbolized as i_{DQ_6}. It is observed that both components of the current have some deviation between the nonlinear and iMTI models trajectories. This deviation is because the initial conditions between the models are not exactly the same and the starting trajectories differ. The figure only extends until the $t = 0.4\,\mathrm{s}$ mark, for better clarity of the initial trajectories. In order to find a set of consistent initial conditions some flexibility must be given, since it is not feasible for Matlab® to match the entire set of initial conditions for both models. For this example, the initial angular deviations of the nonlinear model where enforced to match with the initial value of the $\mathbf{x}_{\mathrm{t}}$ variables in the iMTI model, which lead to slightly different initial value of some states, as is the current from Fig. 5.

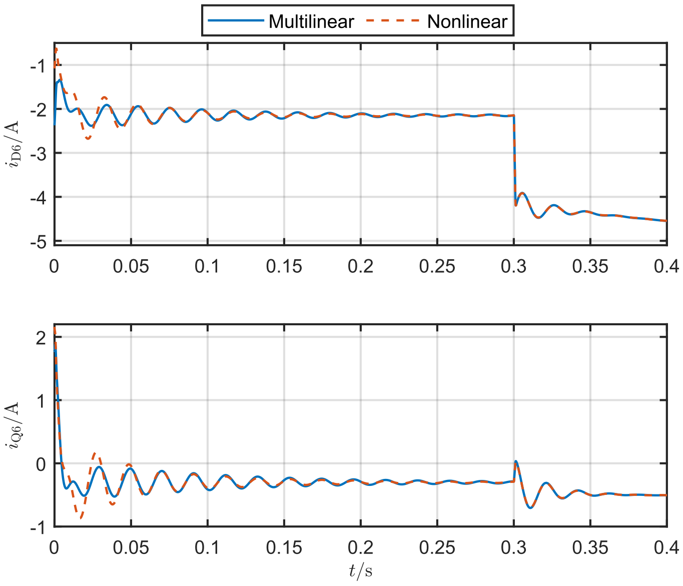

Fig. 5. Line current between busses four and five.

These two figures give an idea of how the models would compare. As long as restrictions such us equations (12) for all inverters stay valid, a deterministic iMTI model can reliability be compared to a deterministic nonlinear model. For this example the restrictions for each inverter where monitored after simulation, which yielded deviations of up to $|4 \times 10^{-9}|$ around 1.

As for storage effort, the required number of elements for this model is linear with the number of states, inputs, equations and equation unique terms. The complete model is stored as CPN1 tensor H_{9b} of rank $r = 651$, according to (5), which requires $\zeta_{CP}(\mathsf{H}_{\mathsf{9b}}) = 610638$ elements. Some additional advantages can be obtained if the CPN1 matrices $\mathbf{H}_s$ and $\mathbf{H}_\phi$, from section III, are stored as sparse matrices.

Finally, the most compelling reduction in storage would result from employing a lower-rank approximation of $\mathbf{H_{9b}}$, which also maintains the sparsity in the tensor, in other words, minimizing the count of unique terms in the approximated set of resulting equations. This aspect remains open for future research, highlighting the significance of sparse-preserving low-rank tensor approximation algorithms.

V. Conclusion

This paper presents a working example of a hybrid iMTI model for a power system network where the model produced an accurate approximation. Reciprocal and trigonometric nonlinearities where lifted by the use of implicit differential equations in order to produce a completely multilinear system of equations. Along with low-rank tensor approximation techniques the multilinear framework shows potential to describe even greater and more complex systems like multi-energy networks. For reproducibility the MTI-toolbox can be used to produce equivalent results, where the complexity of tensor algebra remains partially hidden from the user perspective. Future research must focus on rank reduction strategies that approximate the implicit state transition tensor while preserving sparsity, allowing for significant storage savings at the expense of the iMTI model's desired accuracy.

References

[1] Li, J., Zhang, Y., Fang, H., Fang, S., “Risk evaluation of photovoltaic power systems: An improved failure mode and effect analysis under uncertainty,” J.Clean. Prod. 414, 2023.

[2] Tong, D., Farnham, D.J., Duan, L. et al, “Geophysical constraints on the reliability of solar and wind power worldwide,” Nat Commun 12, 2021.

[3] D. Sampath Kumar, A. Sharma, D. Srinivasan, and T. Reindl, “Impact analysis of large power networks with high share of renewables in transient conditions,” IET Renewable Power Generation 14.8, pp. 1349–1358, 2019.

[4] Guoxuan Cui, Zhongda Chu, and Fei Teng, “Control-mode as a Grid Service in Software-defined Power Grids: GFL vs GFM,” arXiv:2307.15623 [eess.SY], 2023.

[5] Pangalos, G., Eichler, A., and Lichtenberg, G. “Tensor systems - multilinear modeling and applications,” 3rd International Conference on Simulation and Modeling Methodologies, Technologies and Applications (SIMULTECH-2013), pages 275–285., 2013.

[6] Kruppa K., “Multilinear Design of Decentralized Controller Networks for Building Automation Systems,” PhD thesis, Hafen City Universität Hamburg, 2018.

[7] Kruppa K., Pangalos G. , and Lichtenberg G., “Multilinear Approximation of Nonlinear State Space Models,” IFAC Proceedings Volumes 47.3, 2014.

[8] Groß T., Trenn S., and Wirsen A., “Topological solvability and index characterizations for a common DAE power system model,” IEEE Conference on Control Applications (CCA), 2014.

[9] Y. Liu, K. Sun, “Solving Power System Differential Algebraic Equations Using Differential Transformation,” IEEE Power & Energy Society General Meeting (PESGM), 2020.

[10] Groß T., Trenn S., and Wirsen A., “Solvability and stability of a power system DAE model,” Systems & Control Letters, Volume 97, pp. 12-17, 2016.

[11] Kunkel P., Mehrmann V., “Differential-algebraic equations: Analysis and numerical solution,” Vol. 2. European Mathematical Society, 2006.

[12] Mehrmann, V., “Index Concepts for Differential-Algebraic Equations,” Encyclopedia of Applied and Computational Mathematics. Springer, 2015.

[13] Kunkel, P., Mehrmann, V. “Analysis of Over- and Underdetermined Nonlinear Differential-Algebraic Systems with Application to Nonlinear Control Problems,” Math. Control Signals Systems 14, 233–256 , 2001.

[14] Lichtenberg, G. “Hybrid Tensor Systems”, Habilitation, 2011.

[15] Lichtenberg, G., Pangalos, G., Yáñez, C.C., Luxa, A., Jöres, N., Schnelle, L., and Kaufmann C., “Implicit multilinear modeling,” at-Automatisierungstechnik, 70, 13–30, 2022.

[16] Bächle S., “Numerical Solution of Differential-Algebraic Systems Arising in Circuit Simulation,” PhD thesis, Technischen Universität Berlin, 2007.

[17] Höger C., Steinbrecher A., “Internalized state-selection: Generation and integration of quasi-linear differential-algebraic equations,” Proceedings of the 11th International Modelica Conference, pp. 99–107, 2015.

[18] März R., Schwarz D. E., Feldmann U., Sturtzel S., and Tischendorf C., “Finding Beneficial DAE Structures in Circuit Simulation,” Humbold-University Berlin, 2003

[19] Kaufmann C., Pangalos G., Lichtenberg G., and Gomis-Bellmunt O., “Semi-explicit multilinear modeling of a PQ open-loop controlled PV inverter in $\alpha\beta$-frame,” 3rd International Conference on Power, Energy and Electrical Engineering, 2022.

[20] Lichtenberg, G., Eichler, A., “Multilinear Algebraic Boolean Modeling with Tensor Decomposition Techniques”, In Proceedings of the 18th IFAC World Congress, 5603 – 5608, 2011.

[21] Kolda T. G., Bader B. W., “Tensor Decompositions and Applications,” SIAM Review 51.3, pp. 455–500, 2009.

[22] Pogaku N., Prodanovic M., and Green T. C., “Modeling, Analysis and Testing of Autonomous Operation of an Inverter-Based Microgrid,” IEEE Transactions on Power Electronics 22.2, pp. 613–625, 2007.

[23] Kabalan M., Singh P., and Niebur D., “A Design and Optimization Tool for Inverter- Based Microgrids Using Large-Signal Nonlinear Analysis,” IEEE Transactions on Smart Grid 10.4, pp. 4566–4576, 2019.

[24] O'Rourke, C. J., Qasim, M. M., Overlin, M. R., and Kirtley, J. L., “A Geometric Interpretation of Reference Frames and Transformations: dq0, Clarke, and Park,” IEEE Transactions on Energy Conversion 34.4, pp. 2070–2083, 2019.

[25] Samaniego L., “Implicit Multilinear Modeling and Simulation of a medium sized Power System Example,” Master thesis, Hamburg University of Technology, 2023.

[26] Dörfler F., Simpson-Porco J. W., and Bullo F., “Electrical Networks and Algebraic Graph Theory: Models, Properties, and Applications,” Proceedings of the IEEE 106.5, pp. 977–1005, 2018.

[27] Dörfler F., Groß D., “Control of Low-Inertia Power Systems”, Annual Review of Control, Robotics, and Autonomous Systems 6.1, pp. 415-445, 2023.